Face volume densities of positive-intensity and ideal Poisson–Voronoi tessellations in hyperbolic spaces

Matteo D'Achille[a] & Christoph Thäle[b]

Abstract

We determine analytically for all $k \in \{0, 1, \dots, d-1\}$ the k-volume densities of a Poisson–Voronoi tessellation of intensity $\lambda > 0$ in the d-dimensional hyperbolic space of constant curvature -1. This largely extends previous results of Isokawa in dimensions two and three. As applications, we provide closed form expressions for all face volume densities and all typical face volumes of the ideal Poisson–Voronoi tessellation (IPVT), which is the low-intensity limit as $\lambda \downarrow 0$ of the hyperbolic Poisson–Voronoi tessellation. As a main tool we develop a new Blaschke–Petkantschin–type formula in hyperbolic space.

Keywords: Blaschke–Petkantschin formula; hyperbolic geometry; ideal Poisson–Voronoi tessellation (IPVT); k-faces; Poisson–Voronoi tessellation
MSC (2020): 52A55, 60D05, 60G55

1 Introduction and main result

Poisson–Voronoi tessellations and Blaschke–Petkantschin formula in Euclidean spaces. Poisson–Voronoi tessellations are among the most classical models of random spatial subdivision. Starting from a stationary Poisson point process in Euclidean space, one assigns to each point the region consisting of all locations for which this point is the nearest point of the process. This construction produces a random tessellation whose cells describe the domains of influence of the points of the process. Due to its simple definition and rich geometric structure, the Poisson–Voronoi tessellation has become a standard model and has found numerous applications, for instance in materials science, telecommunications, geographical modelling and the analysis of spatial data.
Several fundamental mean values of the Euclidean Poisson–Voronoi tessellation in $\mathbb{R}^d$ are known analytically. These include, in particular, the counting densities of k-faces and the corresponding k-volume densities for all $k \in \{0, 1, \dots, d-1\}$, see [Mø89, Mø94, SW08] and the references mentioned therein. Such formulas are basic quantitative descriptors of the tessellation. They determine how many faces of a given dimension occur per unit volume and how much k-dimensional content these faces carry on average. They therefore provide a benchmark for simulations, a point of comparison

[a]Institut Élie Cartan de Lorraine, CNRS, Université de Lorraine, F-57070, Metz, France.
matteo.d-achille@univ-lorraine.fr
[b]Fakultät für Mathematik, Ruhr-Universität Bochum, D-44801, Bochum, Germany.
christoph.thaele@rub.de

between different random tessellation models, and a starting point for the study of more refined characteristics.

A central role in the derivation of such formulas is played by Blaschke–Petkantschin–type transformations involving spheres. These integral-geometric change-of-variables formulas allow one to separate location, radius and directional information in configuration integrals, and thereby turn geometric characteristics of the tessellation into tractable lower-dimensional integrals. Beyond Poisson–Voronoi tessellations, Blaschke–Petkantschin formulas of this type have become versatile tools in stochastic and computational geometry. We refer to the survey [Nik19], and mention selected applications in [CD18, ENR17, EN18, EN19, RS24].

Poisson–Voronoi tessellations and Blaschke–Petkantschin formula in hyperbolic spaces. It is natural to ask to what extent the analytic theory for Poisson–Voronoi tessellations survives in non-Euclidean geometries. In the present paper we focus on hyperbolic spaces of constant negative curvature -1. Hyperbolic Poisson–Voronoi tessellations retain the basic nearest-neighbour interpretation of their Euclidean counterparts, but the underlying geometry becomes substantially different. In particular, the exponential growth of volume and the absence of a scaling as in Euclidean spaces significantly influence the topology and geometry of the cells, and make explicit computations far more delicate.

Compared with the Euclidean case, considerably fewer characteristics of hyperbolic Poisson–Voronoi tessellations are known in closed form. Detailed studies in dimensions two and three were carried out in [Iso00b, Iso00a], where mean values and structural properties of the corresponding tessellations were investigated based on hyperbolic trigonometry, which is possible only in these low-dimensional cases. In general dimension, first explicit progress was made in [GKT22]. The approach there is based on the relation of hyperbolic Poisson–Voronoi tessellations to so-called beta-star polytopes and yields for any dimension $d \geq 2$ and any $k \in \{0, 1, \dots, d-1\}$ an explicit description of the expected number of k-faces of the typical cell. These numbers determine in turn the k-face counting densities of the hyperbolic Poisson–Voronoi tessellation. However, these results only concern the combinatorial structure of the tessellation. They do not determine the metric size of its lower-dimensional skeletons. In particular, no formula for the k-volume density of the hyperbolic Poisson–Voronoi tessellation in arbitrary dimension seems to have been available so far.

The present paper studies the complementary metric quantity, namely the k-volume density of the hyperbolic Poisson–Voronoi tessellation, in arbitrary dimension. Thus, instead of counting k-faces, we measure their total k-dimensional volume per unit hyperbolic volume. This provides the metric counterpart to the face-counting formulas obtained in [GKT22]. It also substantially extends the explicit computations in low dimensions from [Iso00b, Iso00a] and complements the asymptotic local results of [CCE21] for the face-counting densities of Poisson–Voronoi tessellations on general Riemannian manifolds. The relevance of such metric characteristics is already visible in dimension two: the low-intensity limit of the length density of the one-dimensional skeleton, equivalently the k-volume density for $k = 1$, plays a central role in the upper bound for the Cheeger constant of high genus hyperbolic surfaces obtained in [BCP25]. This connection will be discussed further below in relation to the ideal Poisson–Voronoi tessellation.

A key ingredient in our approach is a new Blaschke–Petkantschin–type formula in hyperbolic

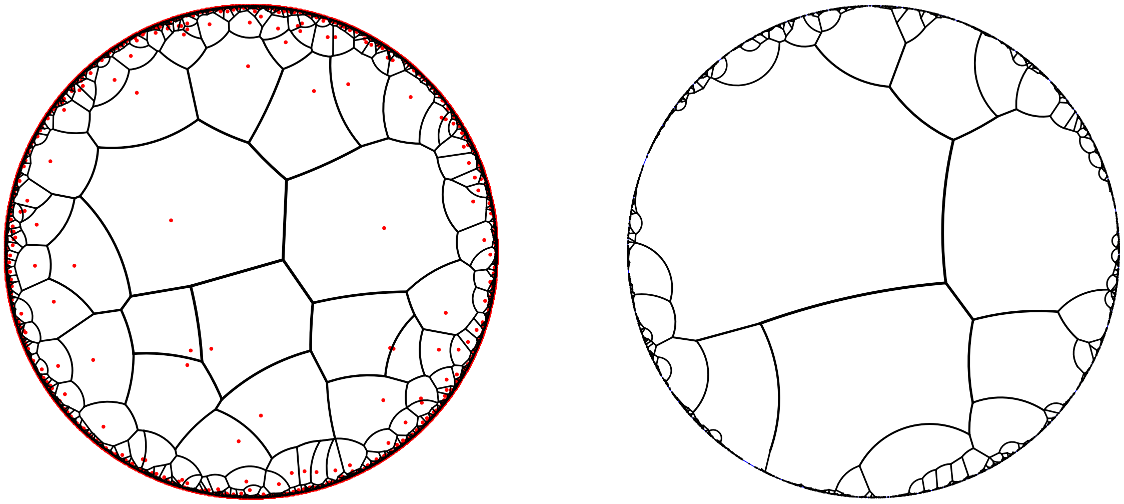

Figure 1.1: Left: sample of the Poisson–Voronoi tessellation of $\mathbb{H}^2$ in the conformal disk model at positive intensity (nuclei in red). Right: sample of $\mathrm{IPVT}(\mathbb{H}^2)$ coupled via dilation from $\mathbf{o}$. In both figures, only the first 10000 nuclei have been used (and displayed in the left one).

space. It decomposes configuration integrals according to the geodesic subspace, the centre and the radius of the circumsphere determined by a collection of points. A boundary case of our formula, corresponding to $d+1$ points with a unique hyperbolic circumcentre, was previously obtained in [Cha18, Proposition 2.1.1]. The form needed here extends this decomposition to lower-dimensional circumspheres and is therefore suited to the analysis of k-faces for every $k \in \{0, 1, \dots, d-1\}$. Since Euclidean Blaschke–Petkantschin formulas of this type have proved to be a versatile tool in the applications discussed above, it is natural to expect that a hyperbolic counterpart will be useful beyond the specific computation carried out here. We therefore regard this formula as an object of independent interest. We moreover mention that the ratio of face-counting densities and face-volume densities available from [Iso00b] has been used in [HM24] to compute the right derivative at $\lambda = 0$ of the critical probability $p_c(\lambda)$ for Poisson–Voronoi percolation on the hyperbolic plane, where the percolation model is defined by colouring independently the cells of a Poisson–Voronoi tessellation with intensity λ. We leave the investigation of the implications of the present work for hyperbolic Poisson–Voronoi percolation in dimensions $d \geq 3$ to future work.

Ideal Poisson–Voronoi tessellations. The explicit formula for the k-volume density of a hyperbolic Poisson–Voronoi tessellation we prove makes it possible to study the low-intensity regime. This connects the present work to the ideal Poisson–Voronoi tessellation (IPVT), a recently introduced limiting object obtained from hyperbolic Poisson–Voronoi tessellations when the number of nuclei per unit volume tends to zero. The ideal Poisson–Voronoi tessellation is a remarkable new scaling limit whose cells are unbounded hyperbolic polytopes with a unique ideal point at infinity. We denote this random tessellation by $\mathrm{IPVT}(\mathbb{H}^d)$, following [DCE+26].

The motivation for ideal Poisson–Voronoi tessellations comes from several directions. They were introduced in part in connection with the study of Cheeger's constant of high genus closed hyperbolic surfaces [BCP25], as alredy indicated above, and are also related to questions on invariant random tessellations and non-amenable geometry, see, for instance, [Bhu19]. Since their introduction, IPVTs and the geometry of their cells have found a number of striking applications. These include connections with Gaboriau's fixed price conjecture [FMW23] and estimates for uniqueness thresholds in Poisson and Bernoulli–Voronoi percolation on product spaces with non-amenable structure [GR25, DGK+25].

For real hyperbolic space $\mathbb{H}^d$, $d \geq 2$, the tessellation $\mathrm{IPVT}\big(\mathbb{H}^d\big)$ is an isometry-invariant random subdivision of $\mathbb{H}^d$ into countably many unbounded hyperbolic polytopes, each having a unique end, see Figure 1.1, right, for a sample in the case $d = 2$. In the upper half-space model, the zero cell, that is, the cell containing an arbitrary but fixed point, admits a particularly transparent description: its law is that of the complement of a union of Euclidean half-balls whose centres and radii are governed by an explicit Poisson point process. This Poissonian representation is one of the central features of the model, and remains available in related non-Euclidean settings beyond $\mathbb{H}^d$, see [D'A24].

As noted above, the face-counting densities of $\mathrm{IPVT}\big(\mathbb{H}^d\big)$ were obtained explicitly in [DCE+26], using the connection with the results of [GKT22]. Combining these formulas with the low-intensity limit of the k-volume densities obtained in the present paper yields corresponding explicit formulas for the mean k-dimensional volume of the typical k-face of the ideal tessellation. Thus our results provide the missing metric counterpart to the known face-counting formulas for IPVTs.

Formulation of the main result. Let $\mathrm{dist}(\cdot,\cdot)$ denote the hyperbolic distance on the d-dimensional hyperbollic space $\mathbb{H}^d$ of constant curvature -1, and let $\mathcal{H}^m$ denote m-dimensional Hausdorff measure, $m \in \{0, 1, \dots, d\}$, with respect to this distance. In particular, $\mathcal{H}^d$ is the hyperbolic volume measure on $\mathbb{H}^d$. Fix $\lambda > 0$, and let η_λ be a Poisson point process on $\mathbb{H}^d$ with intensity measure $\lambda\mathcal{H}^d$. The Voronoi cell with nucleus $x \in \eta_\lambda$ is defined by

$$C(x, \eta_\lambda) = \{y \in \mathbb{H}^d : \mathrm{dist}(y, x) \leq \mathrm{dist}(y, z) \text{ for all } z \in \eta_\lambda\}.$$

The collection of all such cells is the hyperbolic Poisson–Voronoi tessellation with positive intensity λ, see Figure 1.1, left, for a sample in the case $d = 2$. To simplify comparison with the existing literature we remark that in [DCE+26] the intensity was chosen to be λ^{d-1}. For $k \in \{0, 1, \dots, d-1\}$, let $X_k(\eta_\lambda)$ denote the set of all k-faces of this tessellation, that is,

$$X_k(\eta_\lambda) = \bigcup_{x \in \eta_\lambda} \mathcal{F}_k\big(C(x, \eta_\lambda)\big),$$

where $\mathcal{F}_k(P)$ denotes the set of all k-dimensional faces of a polytope P. Fix a bounded Borel set $W \subset \mathbb{H}^d$ with $0 < \mathcal{H}^d(W) < \infty$, and define the k-face volume density by

$$D_{d,k}(\lambda) = \frac{1}{\mathcal{H}^d(W)} \mathbb{E}\left[\sum_{F \in X_k(\eta_\lambda)} \mathcal{H}^k(F \cap W)\right].$$

The expectation on the left-hand side defines an isometry-invariant Radon measure on $\mathbb{H}^d$, and hence is a constant multiple of the hyperbolic volume measure. Thus $D_{d,k}(\lambda)$ is independent of the choice of W. Our first goal is to compute this density explicitly for every positive intensity λ.

Throughout this paper we put $q = d - k$, write

$$\omega_k = \frac{2\pi^{k/2}}{\Gamma(k/2)}$$

for the area of the $(k-1)$-dimensional Euclidean unit sphere, and define

$$A_{d,q} := \frac{\omega_{d(q+1)-q} \cdot \omega_{d+1}^{q} \cdot \omega_{d-q+1}}{\omega_{d(q+1)-q+1}}. \tag{1.1}$$

The constant $A_{d,q}$ has a probabilistic interpretation: $\frac{1}{q!\omega_d^{q+1}} A_{d,q}$ is the expected q-dimensional Euclidean volume of the random simplex generated by $q+1$ independent points sampled uniformly from the Euclidean $(d-1)$-dimensional unit sphere, see [KST26, Chapter 4]. Finally, we denote by

$$b_d(r) = \omega_d \int_0^r \sinh^{d-1}(s)\,\mathrm{d}s, \qquad r > 0,$$

the hyperbolic volume of a hyperbolic ball of radius r.

We are now prepared to present the main result of this paper. It gives a complete analytic formula for all k-face volume densities, $k \in \{0, 1, \dots, d-1\}$, in every dimension $d \geq 2$ and at every positive intensity λ, reducing the problem to a simple explicit one-dimensional radial integral.

Theorem 1.1 (Face volume densities for Poisson–Voronoi tessellations in $\mathbb{H}^d$)**.** *For $d \geq 2$ and $k \in \{0, 1, \dots, d-1\}$, we have, with $q = d - k$,*

$$D_{d,k}(\lambda) = \frac{\lambda^{q+1}}{(q+1)!} A_{d,q} \int_0^\infty \exp\{-\lambda b_d(r)\} \sinh^{(d-1)(q+1)}(r)\,\mathrm{d}r.$$

Remark 1.2. The integral appearing in Theorem 1.1 can be viewed as a Laplace transform. Define

$$\psi(s) = \sinh^{d-1}(b_d^{-1}(s)), \qquad s \geq 0.$$

Then the change of variables $s = b_d(r)$ gives

$$\int_0^\infty \exp\{-\lambda b_d(r)\} \sinh^{(d-1)(q+1)}(r)\,\mathrm{d}r = \omega_d^{-1}\,\mathfrak{L}[\psi^q](\lambda),$$

where $\mathfrak{L}[\psi^q]$ denotes the Laplace transform of the function ψ^q. This observation will be used in the proof of Corollary 2.1 below.

The integral also admits a probabilistic interpretation. If η_λ is an isometry-invariant Poisson process in $\mathbb{H}^d$ with intensity λ, then $\exp\{-\lambda b_d(r)\} = \mathbb{P}\big(\eta_\lambda(B^d_{\mathbb{H}}(\mathbf{o}, r)) = 0\big)$, where $\mathbf{o} \in \mathbb{H}^d$ is fixed. Hence, if R_λ denotes the distance of $\mathbf{o}$ to the nearest point of η_λ, then $\mathbb{P}(R_\lambda > r) = \exp\{-\lambda b_d(r)\}$, or equivalently $b_d(R_\lambda)$ has the exponential distribution with parameter λ. Thus the above integral is the same as

$$\frac{1}{\lambda\omega_d}\,\mathbb{E}\big[\sinh^{q(d-1)}(R_\lambda)\big].$$

Consequently, Theorem 1.1 may also be written as

$$D_{d,k}(\lambda) = \frac{A_{d,q}}{(q+1)!\,\omega_d}\,\lambda^q\,\mathbb{E}\big[\sinh^{q(d-1)}(R_\lambda)\big].$$

Thus the k-face volume density is, up to the constant $A_{d,q}/((q+1)!\,\omega_d)$, determined by the q-th moment of the hyperbolic surface-growth factor at the nearest-neighbour radius of a typical point. This is consistent with the underlying geometric construction: a k-face has codimension q, and locally arises from $q+1$ nuclei on the boundary of an empty hyperbolic ball. The void probability of this ball is $\exp\{-\lambda b_d(r)\}$, while the factor $\sinh^{q(d-1)}(r)$ reflects the remaining q angular degrees of freedom.

	$d=2$	$d=3$	$d=4$
$k=0$	$\frac{1}{\pi}$	$\frac{16\pi}{35}$	$\frac{1287}{16\pi^2}$
$k=1$	$\frac{2}{\pi}$	$\frac{8\pi}{15}$	$\frac{16384}{231\pi^2}$
$k=2$	–	$\frac{4}{3}$	$\frac{105}{8\pi}$
$k=3$	–	–	$\frac{32}{5\pi}$

Table 1: Values of $D_{d,k}$ for $2 \le d \le 4$.

	$d=2$	$d=3$	$d=4$
$k=0$	1	1	1
$k=1$	$\frac{4}{3}$	$\frac{7}{12}$	$\frac{524288}{1486485}$
$k=2$	–	$\frac{35}{12\pi}$	$\frac{7\pi}{85}$
$k=3$	–	–	$\frac{1024\pi}{6075}$

Table 2: Values of $\mathbb{E}\left[\mathcal{H}^k(F_{d,k}^{\mathrm{typ}})\right]$ for $2 \le d \le 4$.

2 Applications to the IPVT

We now turn to the low-intensity regime and its relation with the ideal Poisson–Voronoi tessellation (IPVT). The latter is obtained as the limit in distribution of hyperbolic Poisson–Voronoi tessellations when the intensity λ of the underlying Poisson process tends to zero and was introduced in [DCE+26]. In contrast to the Euclidean case, where changing the intensity merely amounts to a rescaling, the intensity parameter in hyperbolic space has genuine geometric content. Letting $\lambda \downarrow 0$ produces a non-trivial limiting random tessellation, denoted by $\mathrm{IPVT}(\mathbb{H}^d)$, whose cells are unbounded hyperbolic polytopes with exactly one ideal point at infinity. The explicit formula in Theorem 1.1 allows us to compute the low-intensity limit

$$D_{d,k} = \lim_{\lambda \downarrow 0} D_{d,k}(\lambda),$$

which is the k-face volume density of $\mathrm{IPVT}(\mathbb{H}^d)$ according to [DCE+26, Lemma 4.1]. Values for $d \in \{2,3,4\}$ are given in Table 1.

Corollary 2.1 (Face volume densities for $\mathrm{IPVT}(\mathbb{H}^d)$)**.** *For $d \ge 2$ and $k \in \{0,1,\dots,d-1\}$ we have that, with $q = d-k$,*

$$D_{d,k} = \frac{A_{d,q}}{q+1} \frac{(d-1)^q}{\omega_d^{q+1}} .$$

Remark 2.2. To ease comparison with the existing literature, we remark that in [DCE+26], the constant which we call $D_{d,k}$ is denoted by $\tilde{\mathrm{I}}_{d,k}$. In particular, it has been shown in [DCE+26, Proposition 5.3] by computing the slope at the origin of the hole probability for the zero cell of $\mathrm{IPVT}(\mathbb{H}^d)$ that

$$\tilde{\mathrm{I}}_{d,d-1} = \frac{\Gamma(\frac{d}{2})\Gamma(d)}{\Gamma(\frac{d-1}{2})\Gamma(d-\frac{1}{2})} = \frac{d-1}{2} \frac{\omega_{2d-1} \cdot \omega_{d+1}}{\omega_{2d} \cdot \omega_d} .$$

This matches our result for $D_{d,d-1}$.

Remark 2.3. For $d = 2$, the numerical ordering of the face-volume densities is

$$D_{2,0} = \frac{1}{\pi} < \frac{2}{\pi} = D_{2,1}.$$

For $d = 3$, the sequence of the k-volume densities is not monotone, since

$$D_{3,0} = \frac{16\pi}{35} < D_{3,1} = \frac{8\pi}{15} > D_{3,2} = \frac{4}{3}.$$

Starting from dimension $d = 4$, however, the face-volume densities are strictly decreasing in the face dimension. In fact, one can show that $D_{d,0} > D_{d,1} > \ldots > D_{d,d-1}$ for all $d \geq 4$.

We record now several consequences of Corollary 2.1. The first is concerned with the volume of the typical k-face of the IPVT. Using the notation from [DCE+26, Section 4.1], let $\mathrm{I}_{d,k}$ denote the k-face counting density of the IPVT and $D_{d,k}$ denote the corresponding k-volume intensity. While the IPVT does not admit a typical full-dimensional cell in the usual sense, the typical k-face for $k \in \{0, 1, \ldots, d-1\}$ is well defined, since the k-faces of $\mathrm{IPVT}(\mathbb{H}^d)$ are almost surely bounded and have positive and finite counting density. We denote by $F_{d,k}^{\mathrm{typ}}$ the typical k-face of the IPVT, in the sense of the Palm distribution associated with the k-face process, as defined in [DCE+26, Section 4]. Moreover, putting $c(a) = \pi^{-1/2}\,\Gamma(a)/\Gamma(a - 1/2)$, the constant

$$\mathfrak{j}_{d,k} = 2\binom{d}{k} c\Big(\frac{d^2}{2}\Big) \int_0^\infty \cosh^{-(d^2-1)} u\, \Re\Big(\frac{1}{2} + \mathfrak{i}\, c\Big(\frac{d+1}{2}\Big) \int_0^u \cosh^{d-1} v \,\mathrm{d}v\Big)^k \mathrm{d}u$$

is the angle-sum constant appearing in [DCE+26, Equation (4.12)], and

$$\mathrm{IDV}_d = \frac{\pi}{(d-1)^{d+1}} \frac{\omega_d^{d+1} \cdot \omega_{d^2-1}}{\omega_{d+1}^d \cdot \omega_{d^2}}$$

denotes the mean hyperbolic volume of the typical ideal Delaunay simplex. We stress the fact that all these quantities are known analytically from [DCE+26, GKT22, Kab21]. The only missing ingredient for a closed-form expression for $\mathbb{E}\left[\mathcal{H}^k(F_{d,k}^{\mathrm{typ}})\right]$ is therefore the k-volume intensity $D_{d,k}$, which in turn is provided by Corollary 2.1. Combining it with the known formula for the k-face counting density yields the expression below. Some explicit values of $\mathbb{E}\left[\mathcal{H}^k(F_{d,k}^{\mathrm{typ}})\right]$, for $d \in \{2, 3, 4\}$, are displayed in Table 2.

Corollary 2.4 (Mean volumes of typical faces in the IPVT)**.** *For $k \in \{0, 1, \ldots, d-1\}$, with $q = d - k$,*

$$\mathbb{E}\left[\mathcal{H}^k(F_{d,k}^{\mathrm{typ}})\right] = \frac{A_{d,q}\,\mathrm{IDV}_d}{(d+1)\,\mathfrak{j}_{d,k}} \frac{(d-1)^q}{\omega_d^{q+1}}.$$

Corollary 2.1 also has a consequence for ordinary Poisson–Voronoi tessellations of positive intensity in $\mathbb{H}^d$ before passing to the ideal limit. Although the limiting IPVT does not come with a canonical typical cell in the usual Palm sense, the Poisson–Voronoi tessellation with intensity $\lambda > 0$ does. The next corollary shows that the constants $D_{d,k}$ describe the low-intensity blow-up rate of the expected total k-volume of the k-faces of this typical cell.

Corollary 2.5 (Blowup rates for skeletons of the typical Poisson–Voronoi cell)**.** *Let $Z_{d,\lambda}^{\mathrm{typ}}$ denote the typical cell of the Poisson–Voronoi tessellation in $\mathbb{H}^d$ with intensity $\lambda > 0$. Then, for $k \in \{0, 1, \ldots, d-1\}$,*

$$\lim_{\lambda \downarrow 0} \lambda\, \mathbb{E}\Bigg[\sum_{F \in \mathcal{F}_k(Z_{d,\lambda}^{\mathrm{typ}})} \mathcal{H}^k(F)\Bigg] = (d + 1 - k) D_{d,k}.$$

As another application, we mention that the formula in Corollary 2.1 also allows us to read off the behaviour of the k-volume density $D_{d,k}$ of $\mathrm{IPVT}(\mathbb{H}^d)$ in high dimensions, that is, as $d \to \infty$. We only record the main regimes. We use the quotient form of Stirling's formula, which ensures that for fixed $a, b \in \mathbb{R}$,

$$\frac{\Gamma(x+a)}{\Gamma(x+b)} = x^{a-b}\left(1 + \frac{(a-b)(a+b-1)}{2x} + O(x^{-2})\right), \qquad x \to \infty,$$

see [TE51]. Now, if the codimension $q = d - k$ is fixed, then

$$D_{d,d-q} = \frac{d^q}{\sqrt{q+1}}\left(1 - \frac{q(q+2)^2}{4(q+1)d} + O(d^{-2})\right), \qquad d \to \infty.$$

For $q = 1$, this gives $D_{d,d-1} = \frac{d}{\sqrt{2}}(1 - \frac{9}{8d} + O(d^{-2}))$, in agreement with the discussion after Proposition 5.3 in [DCE+26]. If on the other hand $k \geq 0$ is kept fixed, then

$$D_{d,k} = \frac{\omega_{k+1} e^{-3/4}}{\sqrt{2}\,(2\pi)^{k/2}}\, d^{\,d-(k+1)/2} e^{-d/2}\left(1 + \frac{15k-16}{12d} + O(d^{-2})\right), \qquad d \to \infty.$$

In particular, $D_{d,0} = \sqrt{2}\, e^{-3/4}\, d^{d-1/2} e^{-d/2}(1 + O(d^{-1}))$ in agreement with [DCE+26, Theorem 4.7]. Finally, if $k = \alpha d + O(1)$ with $\alpha \in (0,1)$, then Stirling's formula applied on the logarithmic scale leads to

$$\log D_{d,k} = (1-\alpha) d \log d - \frac{1}{2}\,(1 - \alpha + \alpha \log \alpha)\, d + O(\log d)\,.$$

3 Notation and preliminaries

In this section we collect some notation and background material that will be used throughout the paper. The purpose of this section is mainly to provide a common reference point for the geometric conventions we use. Some notation will nevertheless be recalled, or introduced in a more specialized form, at the place where it first becomes relevant. This is meant to keep the main statements readable while still making the technical parts of the paper self-contained.

When we work in the Euclidean space $\mathbb{R}^d$ we write $\|\cdot\|$ for the Euclidean norm and $\langle\cdot,\cdot\rangle$ for the Euclidean scalar product. The dimension will always be clear from the context. We write $B_{\mathbb{R}^d}(z,r) = \{x \in \mathbb{R}^d : \|z - x\| \leq r\}$ and $B^\circ_{\mathbb{R}^d}(z,r) = \{x \in \mathbb{R}^d : \|z - x\| < r\}$ for the closed and open Euclidean balls in $\mathbb{R}^d$ with centre $z \in \mathbb{R}^d$ and radius $r > 0$, respectively. Finally, we write $\omega_d = 2\pi^{d/2}/\Gamma(d/2)$ for the surface measure of the Euclidean unit sphere in $\mathbb{R}^d$.
We denote by $\mathbb{H}^d$ the d-dimensional real hyperbolic space of constant sectional curvature -1, and by $\mathrm{dist}(\cdot,\cdot)$ its geodesic distance. Its Riemannian volume measure is denoted by $\mathcal{H}^d$. Equivalently, this is the d-dimensional Hausdorff measure induced by $\mathrm{dist}(\cdot,\cdot)$. Throughout the paper, $\mathbf{o}$ denotes an arbitrary but fixed point of $\mathbb{H}^d$, which we refer to as the origin. The closed geodesic ball in $\mathbb{H}^d$ with centre x and hyperbolic radius $r > 0$ is denoted by $B_{\mathbb{H}^d}(x,r)$, and the corresponding open ball by $B^\circ_{\mathbb{H}^d}(x,r)$.
More generally, if M is a Riemannian manifold, then, by a slight abuse of notation, $\mathcal{H}^s$, $s \geq 0$, denotes the s-dimensional Hausdorff measure induced by the Riemannian distance on M. For $y \in M$, we write T_yM for the tangent space at y, endowed with the Riemannian inner product $\langle\cdot,\cdot\rangle_y$. Its

unit sphere is denoted by $S_yM = \{u \in T_yM : \langle u, u\rangle_y = 1\}$, and σ_y denotes the spherical Lebesgue measure on S_yM.

For a Riemannian manifold M the exponential map at $y \in M$ is denoted by $\exp_y : T_yM \to M$. Thus, for $u \in S_yM$, the curve $r \mapsto \exp_y(ru)$ is the unit-speed geodesic starting from y in the direction of u, as long as ru belongs to the domain of $\exp_y$. If $x \in M$ does not lie in the cut locus of y, then x has unique geodesic polar coordinates $x = \exp_y(ru)$, where $r > 0$ is the geodesic distance of x to y and $u \in S_yM$. In these coordinates, the Riemannian volume measure is given by $\mathcal{H}^d(\mathrm{d}x) = \mathrm{Jac}_y(r,u)\,\mathrm{d}r\,\sigma_y(\mathrm{d}u)$, where $d = \dim M$ and $\mathrm{Jac}_y(r,u)$ denotes the radial Jacobian of the exponential map. In the case of our interest $M = \mathbb{H}^d$, this Jacobian is independent of y and u, and equals $\sinh^{d-1}(r)$. Thus, in hyperbolic space,

$$\mathcal{H}^d(\mathrm{d}x) = \sinh^{d-1}(r)\,\mathrm{d}r\,\sigma_y(\mathrm{d}u), \qquad x = \exp_y(ru).$$

We refer to [Lee18] for further background material on Riemannian manifolds, especially to [Lee18, Section 5.3] for the exponential map and to [Lee18, Corollary 10.17] for the representation of the volume in $\mathbb{H}^d$ in terms of geodesic polar coordinates.

4 A new Blaschke–Petkantschin–type formula in hyperbolic space

In the proof of Theorem 1.1 we will make use of a new hyperbolic integral-geometric transformation formula of Blaschke–Petkantschin–type, which is in a similar spirit as the transformation formulas developed in [CCE21, Cha18]. To present it, we need some further notation. Let M be an m-dimensional smooth Riemannian manifold, let $1 \le \ell \le m$, and let $F : M \to \mathbb{R}^\ell$ be a smooth map. For a point $z \in M$ put

$$J_F(z) = \sqrt{\det\big(\langle \nabla F_i(z), \nabla F_j(z)\rangle_z\big)_{i,j=1}^{\ell}}, \qquad F = (F_1, \dots, F_\ell).$$

So, J_F is the normal Jacobian of F and $\langle\cdot,\cdot\rangle_z$ denotes the Riemannian inner product in the tangent space T_zM of M at z. We use the same notation for product manifolds.

Proposition 4.1 (Hyperbolic Blaschke–Petkantschin formula)**.** *Let $d \ge 2$, let $k \in \{0, 1, \dots, d-1\}$, and put $q = d - k$. For $\mathbf{x} = (x_0, \dots, x_q) \in (\mathbb{H}^d)^{q+1}$, let*

$$L(\mathbf{x}) = \{y \in \mathbb{H}^d : \mathrm{dist}(y, x_0) = \mathrm{dist}(y, x_1) = \ldots = \mathrm{dist}(y, x_q)\}.$$

For $y \in L(\mathbf{x})$, write $\rho(y, \mathbf{x}) = \mathrm{dist}(y, x_0) = \mathrm{dist}(y, x_1) = \ldots = \mathrm{dist}(y, x_q)$ for the common distance. Then, for every non-negative measurable function $h : \mathbb{H}^d \times [0,\infty) \to [0,\infty]$,

$$\begin{aligned} &\int_{(\mathbb{H}^d)^{q+1}} \int_{L(\mathbf{x})} h\big(y, \rho(y,\mathbf{x})\big)\,\mathcal{H}^k(\mathrm{d}y)\,\mathcal{H}^{d(q+1)}(\mathrm{d}\mathbf{x}) \\ &= A_{d,q} \int_{\mathbb{H}^d} \int_0^\infty h(y, r)\, \sinh^{(d-1)(q+1)}(r)\,\mathrm{d}r\,\mathcal{H}^d(\mathrm{d}y), \end{aligned} \tag{4.1}$$

where $A_{d,q}$ is given by (1.1).

Remark 4.2. (i) The inner integral of the expression on the left-hand side of (4.1) is understood in the almost-everywhere sense. The configurations $\mathbf{x}$ for which $L(\mathbf{x})$ is non-empty but not a smooth k-dimensional submanifold form a $\mathcal{H}^{d(q+1)}$-null set and hence do not affect the value of the integral.

(ii) The case $k = 0$, equivalently $q = d$, is already contained in [Cha18, Proposition 2.1.1]. Indeed, in this case, for every nondegenerate $(d+1)$-tuple of points in $\mathbb{H}^d$, the set $L(\mathbf{x})$ is either empty or consists of a single point. In the latter case, this point is the unique hyperbolic circumcentre. After translating the notation in [Cha18] to curvature -1 and integrating out the angular variables, the formula gives precisely the case $q = d$ of (4.1). Proposition 4.1 shows that the same type of decomposition holds for all $k \in \{0, \dots, d-1\}$.

Proof of Proposition 4.1. Put $\mathbb{X} = (\mathbb{H}^d)^{q+1}$. We consider the set $\mathcal{I} \subset \mathbb{H}^d \times \mathbb{X}$ consisting of all pairs $(y, \mathbf{x})$, with $\mathbf{x} = (x_0, \dots, x_q)$, for which $\operatorname{dist}(y, x_0) = \dots = \operatorname{dist}(y, x_q) > 0$. The part with common radius zero can only occur when $x_0 = \dots = x_q = y$. After projection to $\mathbb{X}$, this is contained in the diagonal $\{x_0 = \dots = x_q\}$, which has $\mathcal{H}^{d(q+1)}$-measure zero. It also gives no contribution to the right-hand side of (4.1), since the singleton $\{0\}$ has zero Lebesgue measure in the radial variable.
We first describe $\mathcal{I}$ as a level set of a suitable function. For that purpose, define

$$F : \mathbb{H}^d \times \mathbb{X} \to \mathbb{R}^q, \qquad (y, \mathbf{x}) \mapsto (F_1(y, \mathbf{x}), \dots, F_q(y, \mathbf{x})),$$

where

$$F_i(y, \mathbf{x}) = \cosh \operatorname{dist}(y, x_i) - \cosh \operatorname{dist}(y, x_0), \qquad i \in \{1, \dots, q\}.$$

The map $(y, x) \mapsto \cosh \operatorname{dist}(y, x)$ is smooth on $\mathbb{H}^d \times \mathbb{H}^d$. Away from the diagonal this follows from the smoothness of the distance function. Near the diagonal, one may use geodesic normal coordinates depending smoothly on the centre x. In these coordinates the function $y \mapsto \cosh \operatorname{dist}(y, x)$ is represented by $v \mapsto \cosh |v|$, which is smooth also at $v = 0$, since it has an even power series (this is the reason why we work with $\cosh \operatorname{dist}(\cdot, \cdot)$ rather than $\operatorname{dist}(\cdot, \cdot)$). Hence, F is smooth on $\mathbb{H}^d \times \mathbb{X}$. Since $r \mapsto \cosh r$ is strictly increasing on $[0, \infty)$, the equation $F(y, \mathbf{x}) = 0$ is equivalent to

$$\operatorname{dist}(y, x_0) = \operatorname{dist}(y, x_1) = \dots = \operatorname{dist}(y, x_q).$$

Thus $\mathcal{I}$ is the part of $F^{-1}(0)$ on which the common distance is positive.
We claim that $\mathcal{I}$ is a smooth submanifold of $\mathbb{H}^d \times \mathbb{X}$. Fix $(y, \mathbf{x}) \in \mathcal{I}$, write the common distance as $r > 0$, and write $x_i = \exp_y(r u_i)$ with $u_i \in S_y \mathbb{H}^d$, $i \in \{0, 1, \dots, q\}$. Consider the derivative of F with respect to the $\mathbb{X}$-variables, keeping y fixed. By the first variation formula for the Riemannian distance [Lee18, Theorem 6.3], $\nabla_x \operatorname{dist}(y, x)$ is the unit vector at x pointing away from y along the geodesic from y to x. Hence $\nabla_x \cosh \operatorname{dist}(y, x) = \sinh \operatorname{dist}(y, x) \nabla_x \operatorname{dist}(y, x)$ and therefore, at a point with $\operatorname{dist}(y, x) = r$ we have $\|\nabla_x \cosh \operatorname{dist}(y, x)\| = \sinh r$. Since the i-th component F_i depends only on x_0 and x_i, we have

$$\nabla_{\mathbf{x}} F_i = \big(-\nabla_{x_0} \cosh \operatorname{dist}(y, x_0), 0, \dots, 0, \nabla_{x_i} \cosh \operatorname{dist}(y, x_i), 0, \dots, 0 \big),$$

and it follows that $\|\nabla_{\mathbf{x}} F_i\|^2 = \sinh^2 r + \sinh^2 r = 2 \sinh^2 r$. This gives the diagonal entries of the Gram matrix. For $i \neq j$ the vectors $\nabla_{\mathbf{x}} F_i$ and $\nabla_{\mathbf{x}} F_j$ have only one common nonzero component, namely the x_0-component. Thus

$$\langle \nabla_{\mathbf{x}} F_i, \nabla_{\mathbf{x}} F_j \rangle_{\mathbf{x}} = \langle -\nabla_{x_0} \cosh \operatorname{dist}(y, x_0), -\nabla_{x_0} \cosh \operatorname{dist}(y, x_0) \rangle_{x_0} = \sinh^2 r,$$

which yields the off-diagonal entries. Summarizing, we see that the Gram matrix of $\nabla_{\mathbf{x}} F_1, \dots, \nabla_{\mathbf{x}} F_q$ is $\sinh^2(r)(I_q + \mathbf{1}\mathbf{1}^\top)$, where $\mathbf{1} = (1, \dots, 1)^\top \in \mathbb{R}^q$ is the vector all whose coordinates are equal to one. Since $\det(I_q + \mathbf{1}\mathbf{1}^\top) = 1 + \mathbf{1}^\top\mathbf{1} = 1 + q$, the determinant of the Gram matrix is $(q+1)\sinh^{2q}(r)$, and therefore the normal Jacobian of $\mathbf{x} \mapsto F(y, \mathbf{x})$ is

$$J_{\mathbf{x}} F(y, \mathbf{x}) = \sqrt{q+1}\,\sinh^q(r). \tag{4.2}$$

In particular, this is strictly positive as soon as $r > 0$, so F is a submersion along $\mathcal{I}$. The implicit function theorem on manifolds shows that $\mathcal{I}$ is a smooth submanifold of dimension $d + (q+1)d - q = d(q+1) + k$, see [Lee13, Chapter 5].

Let $\pi_{\mathbb{X}} : \mathcal{I} \to \mathbb{X}$ and $\pi_{\mathbb{H}^d} : \mathcal{I} \to \mathbb{H}^d$ denote the canonical coordinate projections. We apply the smooth coarea formula for Riemannian manifolds (see [BZ88, Theorem 13.4.2] or (A-2) in the appendix of [How93]) to these two projections. First, applying it to $\pi_{\mathbb{X}}$ gives the left-hand side of (4.1) as an integral over $\mathcal{I}$, namely

$$\int_{\mathbb{X}} \int_{L(\mathbf{x})} h\big(y, \rho(y, \mathbf{x})\big)\, \mathcal{H}^k(\mathrm{d}y)\, \mathcal{H}^{d(q+1)}(\mathrm{d}\mathbf{x}) = \int_{\mathcal{I}} h\big(y, \rho(y, \mathbf{x})\big)\, J_{\pi_{\mathbb{X}}}(y, \mathbf{x})\, \mathcal{H}^{d(q+1)+k}(\mathrm{d}(y, \mathbf{x})),$$

where we recall that $J_{\pi_{\mathbb{X}}}$ denotes the normal Jacobian of the projection $\pi_{\mathbb{X}}$.

We now change the order in which the set $\mathcal{I}$ is sliced. Let J_F denote the normal Jacobian of $F : \mathbb{H}^d \times \mathbb{X} \to \mathbb{R}^q$, and let $J_y F$ and $J_{\mathbf{x}} F$ denote the normal Jacobians of the partial maps obtained by keeping $\mathbf{x}$, respectively y, fixed. On the smooth submanifold $\mathcal{I} \subset F^{-1}(0)$, the normal Jacobians of the restricted coordinate projections satisfy the identities

$$J_{\pi_{\mathbb{X}}}(y, \mathbf{x}) = \frac{J_y F(y, \mathbf{x})}{J_F(y, \mathbf{x})}, \qquad J_{\pi_{\mathbb{H}^d}}(y, \mathbf{x}) = \frac{J_{\mathbf{x}} F(y, \mathbf{x})}{J_F(y, \mathbf{x})},$$

compare with the derivation of Equation (1) in [Zäh90]. These identities follow by applying the smooth coarea formula in local product coordinates to the regular level-set representation of $\mathcal{I}$. Consequently,

$$\frac{J_{\pi_{\mathbb{X}}}(y, \mathbf{x})}{J_{\pi_{\mathbb{H}^d}}(y, \mathbf{x})} = \frac{J_y F(y, \mathbf{x})}{J_{\mathbf{x}} F(y, \mathbf{x})}.$$

Applying the smooth coarea formula to $\pi_{\mathbb{H}^d} : \mathcal{I} \to \mathbb{H}^d$ with the integrand

$$h\big(y, \rho(y, \mathbf{x})\big) \frac{J_{\pi_{\mathbb{X}}}(y, \mathbf{x})}{J_{\pi_{\mathbb{H}^d}}(y, \mathbf{x})}$$

therefore gives

$$\begin{aligned} &\int_{\mathbb{X}} \int_{L(\mathbf{x})} h\big(y, \rho(y, \mathbf{x})\big)\, \mathcal{H}^k(\mathrm{d}y)\, \mathcal{H}^{d(q+1)}(\mathrm{d}\mathbf{x}) \\ &= \int_{\mathbb{H}^d} \int_{\mathcal{I}_y} h\big(y, \rho(y, \mathbf{x})\big)\, \frac{J_y F(y, \mathbf{x})}{J_{\mathbf{x}} F(y, \mathbf{x})}\, \mathcal{H}^{d(q+1)-q}(\mathrm{d}\mathbf{x})\, \mathcal{H}^d(\mathrm{d}y), \end{aligned} \tag{4.3}$$

where $\mathcal{I}_y = \{\mathbf{x} \in \mathbb{X} : (y, \mathbf{x}) \in \mathcal{I}\}$ is the fibre above y.

We now compute the quotient of Jacobians in (4.3). For $(y, \mathbf{x}) \in \mathcal{I}$, write again $x_i = \exp_y(r u_i)$ for $i \in \{0, 1, \ldots, q\}$ with $u_i \in S_y\mathbb{H}^d$ in geodesic polar coordinates around y. As above, by the first variation formula for the Riemannian distance, $\nabla_y F_i(y, \mathbf{x}) = \sinh(r)(u_0 - u_i)$ for $i \in \{1, \ldots, q\}$. Hence,

$$J_y F(y, \mathbf{x}) = \sinh^q(r)\, J(u_0, \ldots, u_q), \qquad J(u_0, \ldots, u_q) \coloneqq \sqrt{\det\big(\langle u_i - u_0, u_j - u_0\rangle_y\big)_{i,j=1}^q}.$$

Together with (4.2), this yields

$$\frac{J_y F(y,\mathbf{x})}{J_{\mathbf{x}} F(y,\mathbf{x})} = \frac{J(u_0,\dots,u_q)}{\sqrt{q+1}}. \tag{4.4}$$

It remains to represent the Hausdorff measure $\mathcal{H}^{d(q+1)-q}$ on $\mathcal{I}_y$ in geodesic polar coordinates. For fixed y, define the map

$$\Phi_y : (0,\infty) \times (S_y\mathbb{H}^d)^{q+1} \to \mathcal{I}_y, (r,u_0,\dots,u_q) \mapsto \big(\exp_y(ru_0),\dots,\exp_y(ru_q)\big).$$

This parametrizes $\mathcal{I}_y$ smoothly and one-to-one, because the exponential map $\exp_y : (0,\infty)\times S_y\mathbb{H}^d \to \mathbb{H}^d \setminus \{y\}$ is a smooth diffeomorphism (there is no cut locus in $\mathbb{H}^d$). For fixed r, the angular map $u_i \mapsto \exp_y(ru_i)$ from $S_y\mathbb{H}^d$ onto the geodesic sphere of radius r has Jacobian $\sinh^{d-1}(r)$ for each $i \in \{0,1,\dots,q\}$. Thus the $q+1$ angular variables contribute the factor

$$\sinh^{(d-1)(q+1)}(r)\,\sigma_y(\mathrm{d}u_0)\cdots\sigma_y(\mathrm{d}u_q).$$

The radial derivative of Φ_y is

$$\partial_r \Phi_y(r,u_0,\dots,u_q) = \Big(\frac{\mathrm{d}}{\mathrm{d}r}\exp_y(ru_0), \frac{\mathrm{d}}{\mathrm{d}r}\exp_y(ru_1),\dots,\frac{\mathrm{d}}{\mathrm{d}r}\exp_y(ru_q)\Big).$$

Each component is the velocity vector of a unit-speed geodesic and thus has unit length. Since the components lie in mutually orthogonal factors of the product $(\mathbb{H}^d)^{q+1}$, it follows that

$$\big\|\partial_r\Phi_y\big\|^2 = \sum_{i=0}^{q}\Big\|\frac{\mathrm{d}}{\mathrm{d}r}\exp_y(ru_i)\Big\|^2 = q+1$$

Moreover, the radial direction is orthogonal to all angular directions in the product tangent space $T_{\mathbf{x}}\mathbb{X}$, where $\mathbf{x} = \Phi_y(r,u_0,\dots,u_q)$. Hence the Jacobian of Φ_y is $\sqrt{q+1}\,\sinh^{(d-1)(q+1)}(r)$, and therefore

$$\mathcal{H}^{d(q+1)-q}(\mathrm{d}\mathbf{x}) = \sqrt{q+1}\,\sinh^{(d-1)(q+1)}(r)\,\mathrm{d}r\,\sigma_y(\mathrm{d}u_0)\cdots\sigma_y(\mathrm{d}u_q).$$

Substituting the last identity and (4.4) into (4.3), the factors $\sqrt{q+1}$ cancel, and we obtain

$$\begin{aligned}&\int_{\mathbb{X}}\int_{L(\mathbf{x})} h\big(y,\rho(y,\mathbf{x})\big)\,\mathcal{H}^k(\mathrm{d}y)\,\mathcal{H}^{d(q+1)}(\mathrm{d}\mathbf{x})\\ &= \int_{\mathbb{H}^d}\int_{(S_y\mathbb{H}^d)^{q+1}}\int_0^\infty h(y,r)\,J(u_0,\dots,u_q)\,\sinh^{(d-1)(q+1)}(r)\,\mathrm{d}r\,\sigma_y(\mathrm{d}u_0)\cdots\sigma_y(\mathrm{d}u_q)\,\mathcal{H}^d(\mathrm{d}y).\end{aligned} \tag{4.5}$$

It remains only to evaluate the $(q+1)$-fold integral over $S_y\mathbb{H}^d$. After identifying $T_y\mathbb{H}^d$ isometrically with $\mathbb{R}^d$, we have $J(u_0,\dots,u_q) = q!\Delta_q(u_0,\dots,u_q)$, where $\Delta_q(u_0,\dots,u_q)$ denotes the Euclidean q-dimensional volume of the simplex with vertices $u_0,\dots,u_q$. Hence, by the spherical simplex moment formula, see [SW08, Theorem 8.2.3] and [KST26, Theorem 4.12],

$$\int_{(S_y\mathbb{H}^d)^{q+1}} J(u_0,\dots,u_q)\,\sigma_y(\mathrm{d}u_0)\cdots\sigma_y(\mathrm{d}u_q) = A_{d,q}.$$

The left-hand side is independent of y, by rotational invariance. Combining this identity with (4.5) proves (4.1). □

5 Proof of Theorem 1.1

Fix $d \geq 2$, $k \in \{0, 1, \dots, d-1\}$ and put $q = d - k$. We write $\eta_{\lambda,\neq}^{q+1}$ for the collection of ordered $(q+1)$-tuples of points of the Poisson point process η_λ. For $\mathbf{x} = (x_0, \dots, x_q) \in \eta_{\lambda,\neq}^{q+1}$ write

$$L(\mathbf{x}) = \{y \in \mathbb{H}^d : \mathrm{dist}(y, x_0) = \mathrm{dist}(y, x_1) = \ldots = \mathrm{dist}(y, x_q)\},$$

and $\rho(y, \mathbf{x}) = \mathrm{dist}(y, x_0)$ for the common distance. We first work on the full-probability event on which the Poisson–Voronoi tessellation is normal. Thus no point of $\mathbb{H}^d$ is equidistant from more than $d+1$ nuclei, and, for $q = d-k$, the relative interior of each k-face is generated by a unique unordered $(q+1)$-tuple of nuclei. More precisely, if $\mathbf{x} = (x_0, \dots, x_q)$ is such a tuple, then the corresponding relative interior consists of those points $y \in L(\mathbf{x})$ for which $\eta_\lambda \cap B^\circ_{\mathbb{H}^d}(y, \rho(y, \mathbf{x})) = \emptyset$. The remaining points belong to lower-dimensional faces and therefore do not contribute to the k-dimensional Hausdorff measure. Hence, for every bounded Borel set $W \subset \mathbb{H}^d$ with $0 < \mathcal{H}^d(W) < \infty$,

$$\sum_{F \in X_k(\eta_\lambda)} \mathcal{H}^k(F \cap W) = \frac{1}{(q+1)!} \sum_{(x_0,\dots,x_q) \in \eta_{\lambda,\neq}^{q+1}} \int_{L(\mathbf{x}) \cap W} \mathbf{1}\{\eta_\lambda \cap B^\circ_{\mathbb{H}^d}(y, \rho(y, \mathbf{x})) = \varnothing\} \, \mathcal{H}^k(\mathrm{d}y), \quad (5.1)$$

where the factor $(q+1)!$ removes the ordering of the same generating $(q+1)$-tuple of nuclei. Taking expectations and applying the multivariate Mecke equation in [SW08, Corollary 3.2.3] gives

$$D_{d,k}(\lambda) = \frac{\lambda^{q+1}}{(q+1)! \, \mathcal{H}^d(W)} \int_{(\mathbb{H}^d)^{q+1}} \int_{L(\mathbf{x}) \cap W} \mathbb{P}\{\eta_\lambda \cap B^\circ_{\mathbb{H}^d}(y, \rho(y, \mathbf{x})) = \varnothing\} \, \mathcal{H}^k(\mathrm{d}y) \mathcal{H}^{d(q+1)}(\mathrm{d}\mathbf{x}).$$

Next, we use the Poisson void probability together with the fact that the volume of a hyperbolic ball only depends on its radius. This gives

$$D_{d,k}(\lambda) = \frac{\lambda^{q+1}}{(q+1)! \, \mathcal{H}^d(W)} \int_{(\mathbb{H}^d)^{q+1}} \int_{L(\mathbf{x}) \cap W} \exp\{-\lambda b_d(\rho(y, \mathbf{x}))\} \, \mathcal{H}^k(\mathrm{d}y) \mathcal{H}^{d(q+1)}(\mathrm{d}\mathbf{x}). \quad (5.2)$$

We now apply Proposition 4.1 to the right-hand side of (5.2). Recall that, for $\mathbf{x} = (x_0, \dots, x_q) \in (\mathbb{H}^d)^{q+1}$, the set $L(\mathbf{x})$ consists of all points $y \in \mathbb{H}^d$ having the same distance from $x_0, \dots, x_q$. Define the non-negative measurable function

$$h_\lambda : \mathbb{H}^d \times [0, \infty) \to [0, \infty], (y, r) \mapsto \mathbf{1}_W(y) \exp\{-\lambda b_d(r)\}.$$

Then the integral in (5.2) can be written as

$$\int_{(\mathbb{H}^d)^{q+1}} \int_{L(\mathbf{x})} h_\lambda\big(y, \rho(y, \mathbf{x})\big) \, \mathcal{H}^k(\mathrm{d}y) \, \mathcal{H}^{d(q+1)}(\mathrm{d}\mathbf{x}).$$

By Proposition 4.1, applied to h_λ, we obtain

$$\begin{aligned}
&\int_{(\mathbb{H}^d)^{q+1}} \int_{L(\mathbf{x})} h_\lambda\big(y, \rho(y, \mathbf{x})\big) \, \mathcal{H}^k(\mathrm{d}y) \, \mathcal{H}^{d(q+1)}(\mathrm{d}\mathbf{x}) \\
&= A_{d,q} \int_{\mathbb{H}^d} \int_0^\infty h_\lambda(y, r) \, \sinh^{(d-1)(q+1)}(r) \, \mathrm{d}r \, \mathcal{H}^d(\mathrm{d}y) \\
&= A_{d,q} \int_{\mathbb{H}^d} \mathbf{1}_W(y) \, \mathcal{H}^d(\mathrm{d}y) \int_0^\infty \exp\{-\lambda b_d(r)\} \sinh^{(d-1)(q+1)}(r) \, \mathrm{d}r \\
&= A_{d,q} \, \mathcal{H}^d(W) \int_0^\infty \exp\{-\lambda b_d(r)\} \sinh^{(d-1)(q+1)}(r) \, \mathrm{d}r,
\end{aligned}$$

where we also used Fubini's theorem. Consequently,

$$D_{d,k}(\lambda) = \frac{A_{d,q}\lambda^{q+1}}{(q+1)!} \int_0^\infty \exp\{-\lambda b_d(r)\} \sinh^{(d-1)(q+1)}(r)\, \mathrm{d}r. \tag{5.3}$$

This completes the proof of Theorem 1.1. □

6 Proofs of the Corollaries for the IPVT

Proof of Corollary 2.1. We identify the limit of $D_{d,k}(\lambda)$ as $\lambda \downarrow 0$. We use the formula from Theorem 1.1 and put for ease of notation

$$I_\lambda := \lambda^{q+1} \int_0^\infty \exp\{-\lambda b_d(r)\} \sinh^{(d-1)(q+1)}(r)\, \mathrm{d}r.$$

By Remark 1.2,

$$I_\lambda = \frac{\lambda^{q+1}}{\omega_d} \mathfrak{L}[\psi^q](\lambda), \qquad \psi(s) = \sinh^{d-1}\big(b_d^{-1}(s)\big).$$

Moreover, the large-radius asymptotics for the volume of hyperbolic balls gives

$$b_d(r) = \omega_d \int_0^r \sinh^{d-1}(t)\, \mathrm{d}t \sim \frac{\omega_d}{d-1} \sinh^{d-1}(r), \qquad r \to \infty,$$

and hence

$$\psi(s)^q \sim \left(\frac{d-1}{\omega_d}\right)^q s^q, \qquad s \to \infty,$$

where the notation $\sim$ indicates that the ratio of the left- and the right-hand side tends to 1. Thus ψ^q is regularly varying at infinity with index q. Karamata's Abelian theorem for Laplace transforms [Fel71, Chapter XIII.5, Theorem 5] therefore yields

$$\mathfrak{L}[\psi^q](\lambda) \sim \left(\frac{d-1}{\omega_d}\right)^q \Gamma(q+1)\lambda^{-(q+1)}, \qquad \lambda \downarrow 0.$$

Consequently,

$$I_\lambda \longrightarrow q!\, \frac{(d-1)^q}{\omega_d^{q+1}}, \qquad \lambda \downarrow 0.$$

Combining this with the representation of $D_{d,k}(\lambda)$, we obtain

$$D_{d,k} = \lim_{\lambda \downarrow 0} D_{d,k}(\lambda) = \frac{A_{d,q}}{(q+1)!}\, q!\, \frac{(d-1)^q}{\omega_d^{q+1}} = \frac{A_{d,q}}{q+1}\, \frac{(d-1)^q}{\omega_d^{q+1}}.$$

This completes the proof. □

Proof of Corollary 2.4. By [DCE+26, Proposition 4.2],

$$\mathbb{E}\left[\mathcal{H}^k(F_{d,k}^{\mathrm{typ}})\right] = \frac{D_{d,k}}{\mathrm{I}_{d,k}},$$

, where we recall that $\mathrm{I}_{d,k}$ denotes the k-face counting density in $\mathrm{IPVT}\big(\mathbb{H}^d\big)$. The statement follows now by combining the result of Corollary 2.1 with

$$\mathrm{I}_{d,k} = \frac{d+1}{q+1}\, \frac{\mathrm{j}_{d,k}}{\mathrm{IDV}_d}$$

from [DCE+26, Theorem 4.7]. □

Proof of Corollary 2.5. For a normal isometry-invariant tessellation of $\mathbb{H}^d$, the balance relation between the typical cell and the k-face volume intensity gives

$$\mathbb{E}\left[\sum_{F\in\mathcal{F}_k(Z_{d,\lambda}^{\mathrm{typ}})}\mathcal{H}^k(F)\right]=\frac{d+1-k}{\lambda}\,D_{d,k}(\lambda).$$

Indeed, by normality every k-face is almost surely incident to exactly $d+1-k$ full-dimensional cells, and the cell intensity is λ, see [DCE$^+$26, Proposition 4.3]. Multiplying by λ and using $D_{d,k}(\lambda)\to D_{d,k}$ as $\lambda\downarrow 0$, yields the claim. □

Acknowledgements. We would like to thank Pierre Calka for bringing the dissertation [Cha18] to our attention. M.D'A. acknowledges support by the ANR project *LOUCCOUM* (ANR-24-CE40-7809). CT was supported by the DFG via SPP 2265 *Random Geometric Systems*. This work was initiated during the Mini-Workshop *Hyperbolic Meets Stochastic Geometry* at the Mathematisches Forschungsinstitut Oberwolfach (MFO), see [KT26]. M.D'A. is grateful to the Department of Mathematics of Ruhr University Bochum for excellent working conditions in the occasion of an invitation during which this work has been partly done. The authors used ChatGPT as a writing and discussion tool in preparing the manuscript. The mathematical content is the responsibility of the authors.

References

[BCP25] Thomas Budzinski, Nicolas Curien, and Bram Petri. On Cheeger constants of hyperbolic surfaces. *Inventiones mathematicae*, 242(2):511–530, 2025.

[Bhu19] Sandeep Bhupatiraju. *The Low–Intensity Limit of Bernoulli–Voronoi and Poisson–Voronoi measures*. PhD thesis, Indiana University, Bloomington, 2019. Available at https://hdl.handle.net/2022/29005.

[BZ88] Yuri D. Burago and Viktor A. Zalgaller. *Geometric Inequalities*, volume 285 of *Grundlehren der mathematischen Wissenschaften [Fundamental Principles of Mathematical Sciences]*. Springer-Verlag, Berlin, 1988. Translated from the Russian by A. B. Sosinskiĭ, Springer Series in Soviet Mathematics.

[CCE21] Pierre Calka, Aurélie Chapron, and Nathanaël Enriquez. Poisson–Voronoi tessellation on a Riemannian manifold. *International Mathematics Research Notices*, 2021(7):5413—5459, 2021.

[CD18] Nicolas Chenavier and Olivier Devillers. Stretch factor in a planar Poisson-Delaunay triangulation with a large intensity. *Adv. in Appl. Probab.*, 50(1):35–56, 2018.

[Cha18] Aurélie Chapron. *Mosaïques de Poisson–Voronoï sur une variété riemannienne*. PhD thesis, Université Paris Nanterre, 2018. Available at https://theses.fr/2018PA100098/document.

[D'A24] Matteo D'Achille. Ideal Poisson–Voronoi tessellations beyond hyperbolic spaces. *arXiv preprint:2412.00822*, 2024. Available at http://arxiv.org/abs/2412.00822.

[DCE+26] Matteo D'Achille, Nicolas Curien, Nathanaël Enriquez, Russell Lyons, and Meltem Ünel. Ideal Poisson–Voronoi tessellations on hyperbolic spaces. *The Annals of Probability*, 54(2):846–891, 2026.

[DGK+25] Matteo D'Achille, Jan Grebík, Ali Khezeli, Konstantin Recke, and Amanda Wilkens. Vanishing uniqueness thresholds in Voronoi percolation on products. *arXiv preprint arXiv:2511.23317*, 2025. Available at http://arxiv.org/abs/2511.23317.

[EN18] Herbert Edelsbrunner and Anton Nikitenko. Random inscribed polytopes have similar radius functions as Poisson-Delaunay mosaics. *Ann. Appl. Probab.*, 28(5):3215–3238, 2018.

[EN19] Herbert Edelsbrunner and Anton Nikitenko. Weighted Poisson-Delaunay mosaics. *Teor. Veroyatn. Primen.*, 64(4):746–770, 2019.

[ENR17] Herbert Edelsbrunner, Anton Nikitenko, and Matthias Reitzner. Expected sizes of Poisson-Delaunay mosaics and their discrete Morse functions. *Adv. in Appl. Probab.*, 49(3):745–767, 2017.

[Fel71] William Feller. *An Introduction to Probability Theory and its Applications. Vol. II.* John Wiley & Sons, New York, second edition, 1971.

[FMW23] Mikolaj Fraczyk, Sam Mellick, and Amanda Wilkens. Poisson–Voronoi tessellations and fixed price in higher rank. *arXiv preprint:2307.01194*, 2023. To appear on Ann. of Math. Available at http://arxiv.org/abs/2307.01194.

[GKT22] Thomas Godland, Zakhar Kabluchko, and Christoph Thäle. Beta-star polytopes and hyperbolic stochastic geometry. *Adv. Math.*, 404:Paper No. 108382, 69, 2022.

[GR25] Jan Grebík and Konstantin Recke. Poisson–Voronoi percolation in higher rank. *arXiv preprint arXiv:2504.02435*, 2025. Available at http://arxiv.org/abs/2504.02435.

[HM24] Benjamin Hansen and Tobias Müller. Poisson–Voronoi percolation in the hyperbolic plane with small intensities. *The Annals of Probability*, 52(6):2342–2405, 2024.

[How93] Ralph Howard. *The Kinematic Formula in Riemannian Homogeneous Spaces*, volume 106 of *Memoirs of the American Mathematical Society*. American Mathematical Society, Providence, RI, 1993.

[Iso00a] Yukinao Isokawa. Poisson-Voronoi tessellations in three-dimensional hyperbolic spaces. *Adv. in Appl. Probab.*, 32(3):648–662, 2000.

[Iso00b] Yukinao Isokawa. Some mean characteristics of Poisson-Voronoi and Poisson-Delaunay tessellations in hyperbolic planes. *Bull. Fac. Ed. Kagoshima Univ. Natur. Sci.*, 52:11–25, 2000.

[Kab21] Zakhar Kabluchko. Angles of random simplices and face numbers of random polytopes. *Adv. Math.*, 380:Paper No. 107612, 68, 2021.

[KST26] Zakhar Kabluchko, David Albert Steigenberger, and Christoph Thäle. *Random Simplices*, volume 2383 of *Lecture Notes in Mathematics*. Springer, Cham, 2026.

[KT26] Ruth Kellerhals and Christoph Thäle. Mini-workshop: Hyperbolic meets stochastic geometry. *Oberwolfach Reports*, 22(4):3031–3062, 2026.

[Lee13] John M. Lee. *Introduction to Smooth Manifolds*, volume 218 of *Graduate Texts in Mathematics*. Springer, New York, second edition, 2013.

[Lee18] John M. Lee. *Introduction to Riemannian manifolds*, volume 2. Springer, 2018.

[Mø89] Jesper Møller. Random tessellations in $\mathbf{R}^d$. *Adv. in Appl. Probab.*, 21(1):37–73, 1989.

[Mø94] Jesper Møller. *Lectures on random Voronoĭ tessellations*, volume 87 of *Lecture Notes in Statistics*. Springer-Verlag, New York, 1994.

[Nik19] Anton Nikitenko. Integrating by spheres: summary of Blaschke-Petkantschin formulas. *arXiv e-prints*, page arXiv:1904.10750, April 2019. Available at http://arxiv.org/abs/1904.10750.

[RS24] Matthias Reitzner and Anna Strotmann. Poisson–Delaunay approximation. *arXiv e-prints*, page arXiv:2410.23003, October 2024. Available at http://arxiv.org/abs/2410.23003.

[SW08] Rolf Schneider and Wolfgang Weil. *Stochastic and Integral Geometry*. Probability and its Applications (New York). Springer-Verlag, Berlin, 2008.

[TE51] Francesco G. Tricomi and Arthur Erdélyi. The asymptotic expansion of a ratio of gamma functions. *Pacific Journal of Mathematics*, 1(1):133–142, 1951.

[Zäh90] Martina Zähle. A kinematic formula and moment measures of random sets. *Mathematische Nachrichten*, 149(1):325–340, 1990.